Supporting Information

Cyclen molecule manipulation for efficient and stable perovskite solar cells

Yuyao Yang,[a#] Li Yuan,[a#] Qing Chang,[b#] Yang Yang,[a] Xiongkai Tang,[b] Zhi Wan,[a] Jieru Du,[a] Hang Wei,[a] Chong Liu,[a] Pengfei Guo,[a] Zhe Liu,[*a] Ruihao Chen,[*a] Hongqiang Wang[*a]

a. State Key Laboratory of Solidification Processing, Center for Nano Energy Materials, School of Materials Science and Engineering, Northwestern Polytechnical University and Shaanxi Joint Laboratory of Graphene, Xi'an 710072, China

b. Pen-Tung Sah Institute of Micro-Nano Science and Technology, College of Chemistry and Chemical Engineering, Xiamen University, Xiamen, 361005, China

* Corresponding authors.

E-mail: rhchen@nwpu.edu.cn, zhe.liu@nwpu.edu.cn, hongqiang.wang@nwpu.edu.cn

Experimental Section

Materials

Cyclen (Alfa Aesar, 99.88%), Cyclen (99.88%) and Cyclam (99%) were purchased from Alfa Aesar and Innochem, respectively. PbI_2 (>9 9.99%), MACl (99.50%), FAI (99.50%), CsI (99.50%), MABr (99.50%), Spiro-OMeTAD (> 99.80%), Li-TFSI (> 99.90%), Co-TFSI (> 99.90%) and tBP (> 99.90%) were purchased from p-OLED. FTO (14 Ω sq^{-1}) were purchased from Advanced Election Technology Co., Ltd. DMF (99.80%), DMSO (99.80%), EA (99.80%), IPA (99.80%) and CB (99.80%) were purchased from Sigma-Aldrich.

Device fabrication

The device configuration of FTO/TiO_2/perovskite/Spiro-OMeTAD/Ag were used, wherein the FTO was the bottom layer. The process for fabricating the device is summarized as follow: The etched FTO substrate was sequentially cleaned with detergent (once), deionized water (twice), IPA (twice) and ethanol (once) in an ultrasonic bath for 40 min. The cleaned FTO substrate was then further treated by ultraviolet light–ozone for 15 min to increase wettability. After that, a 50-nm-thick TiO_2 layer was fabricated by a chemical bath method[1]. For depositing the perovskite layer, a mixture solution of PbI_2 (742.2 mg), FAI ($CH(NH_2)_2I$, 224.4 mg), MABr (CH_3NH_3Br, 16.2 mg), MACl (CH_3NH_3I, 20.3 mg), CsI (19.8 mg) and cyclen (with different concentration) in DMF/DMSO (4:1 v/v) was spun on the FTO/TiO_2 substrate at 4000 rpm for 30 s, and then 200 μL EA was dropped on above spinning substrate at 10 s prior the end of the process, and then the film was heat-treated at 130 °C for 10 min. The fabrication process of $FAPbI_3$ film was referred to previous work[2]. The Spiro-OMeTAD and the Ag or Au electrodes was subsequently deposited[3]. The active area is 0.05 cm^2 by a mask.

For the fabrication of solar modules, to verify the universality of cyclen molecules, we used thermal-stable FACs perovskite to prepare the module. The FACs perovskite precursor is a mixture solution of PbI_2 (461 mg), FAI (163.4 mg), $PbCl_2$ (19.2 mg), MACl (20 mg), CsI (13 mg) and cyclen (0.2 mg/mL) in 600 μL DMF and 90 μL DMSO. The large-scale perovskite layers were prepared by the blade coating and a vacuum-flash process. The gap between the blade and the FTO/TiO_2 was about 200 μm and the speed of the blade was 5 mm s^{-1}. Subsequently the wet film was shifted into a vacuum system to quickly remove solvent. The vacuum-flash process is carried out by the following: after the blade-coating process, the obtained wet film was shifted in a small vacuum chamber. Under the action of a vacuum pump, the pressure in the chamber was rapidly reduced to ~ 10 Pa within 10 s, and then maintained for 15 s at this pressure. Subsequently, the film was shifted onto a hotplate for 10 min annealing at 130 ^oC. For the P1-P3 laser-patterning lines and the remaining process were according to the

previous work[4].

Characterization

The diffraction data of cyclen-PbI_2-DMSO crystals were collected by an X ray single crystal diffractometer (Rigaku Oxford Diffraction system) and the data were processed using CrysAlisPro. The CCDC number of cyclen-PbI_2-DMSO crystallographic data is 2221271. The absorption of perovskite films was test by UV-vis spectrophotometer (Shimadzu UV-2550). Morphology of the films and devices was tested on a scanning electron microscope. The PL and TRPL (excitation at 470 nm) spectra were obtained using a Pico Quant Fluo Time300 fluorescence spectrometer. The current–voltage (*J-V*) curves characteristics were measured under 100 mW cm^{-2} (AM 1.5G illumination) calibrated by a certified reference solar cell in an Enli Technology solar simulator (IVS-KA5000) and a Keithley 2420 source/meter. The EQE spectra were measured by an Enli Technology EQE measurement system. The steady-state power out measurement of PSCs were measured using the Keithley 2420 source meter under 100 mW cm^{-2} (AM 1.5G illumination) with a bias voltage. For the moisture stability tests, nonencapsulated PSCs were performed at 60% RH and room temperature environment. The thermal-stability of the nonencapsulated PSCs were put on a hot plate (85 °C) in a glovebox (N_2 atmosphere) and the Spiro-OMeTAD hole transport layer (HTM) was replaced by PTAA to achieve better stability. The light-stability of the unsealed PSCs were tested under AM 1.5G illumination in N_2 atmosphere. The first-principles calculations were referred to our previous work[4].

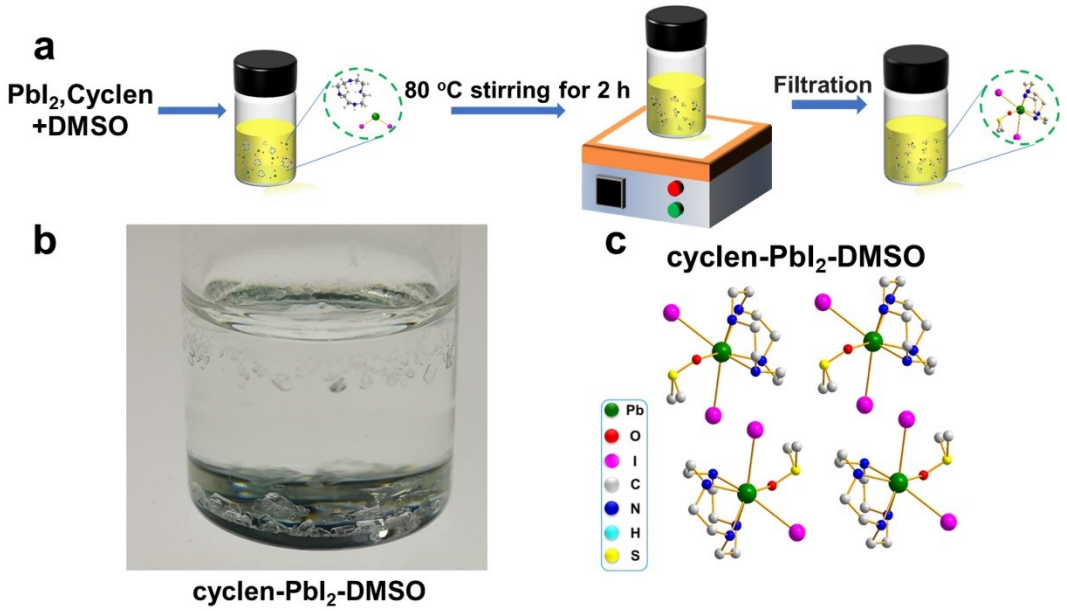

Figure S1. (a) Schematic diagrams of perovskite solution preparation. (b) Photographs and (c) structure of cyclen-PbI_2-DMSO crystals.

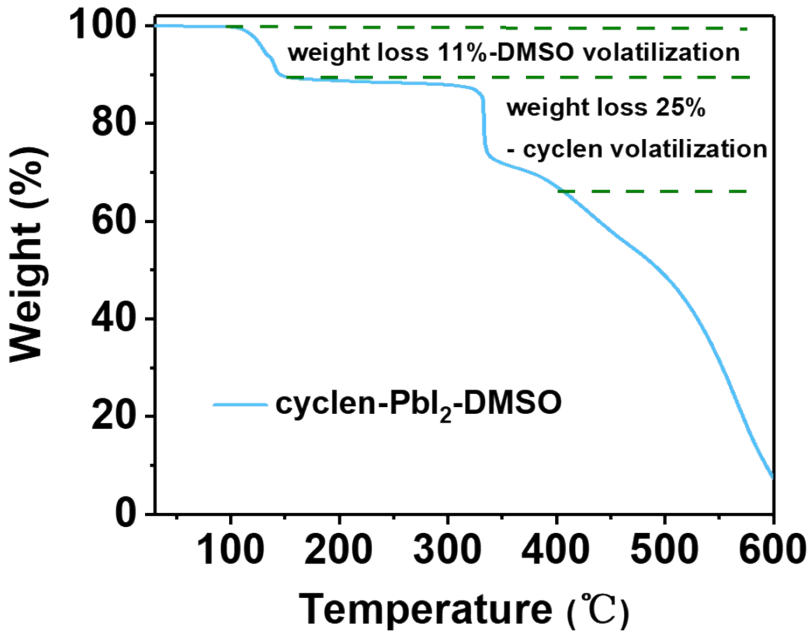

Figure S2. Thermogravimetry (TG) analysis of cyclen-PbI_2-DMSO crystals under Ar atmosphere.

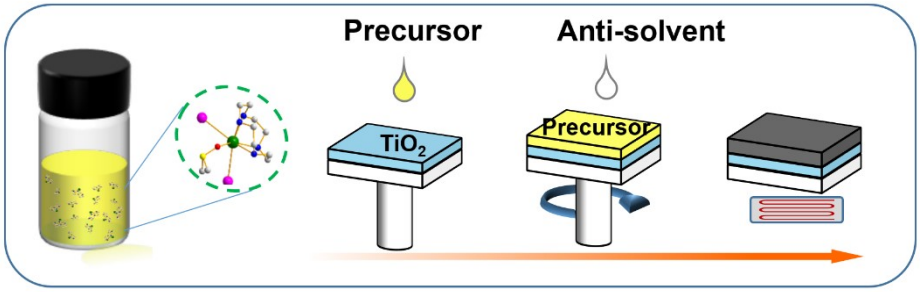

Figure S3. Schematic illustration of perovskite films by spin coating.

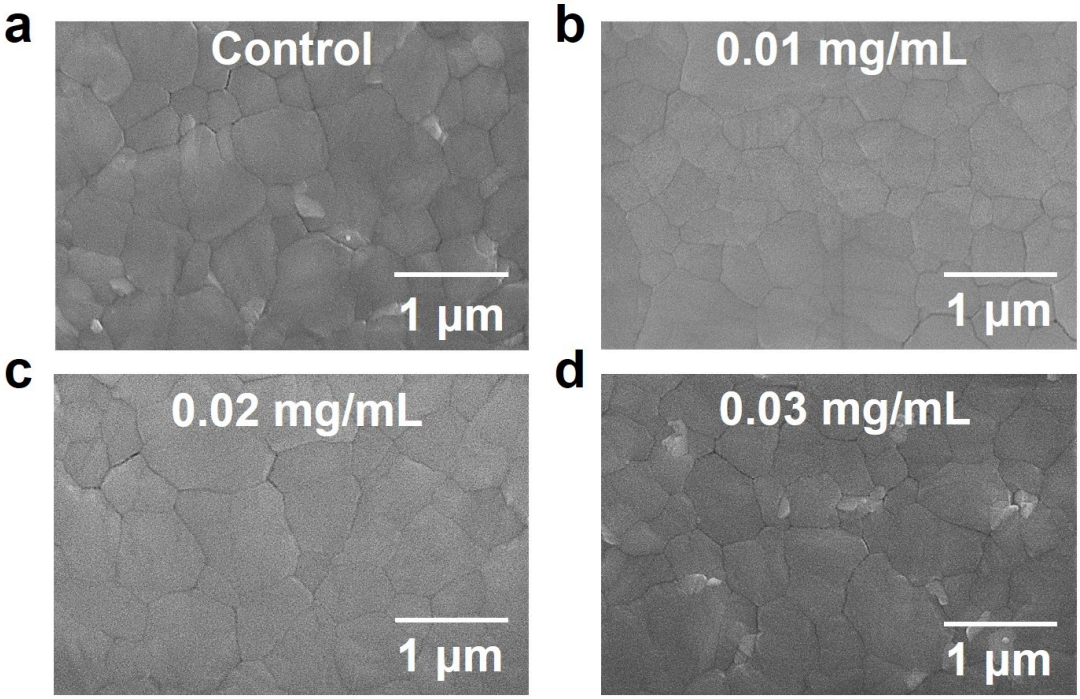

Figure S4. SEM images of the perovskite films without (a) and with different concentrations of cyclen (b) 0.01 mg/mL; (c) 0.02 mg/mL; (d) 0.03 mg/mL.

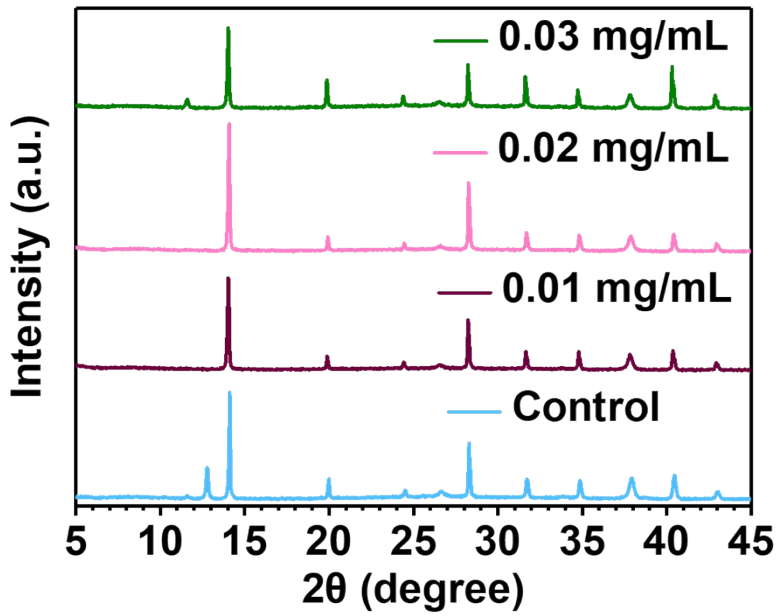

Figure S5. XRD patterns of the perovskite films without and with different concentrations of cyclen.

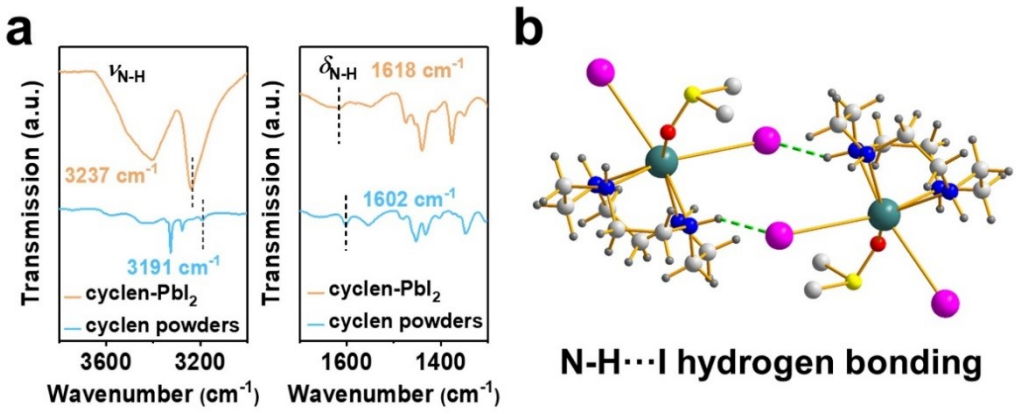

Figure S6. (a) FTIR spectra of cyclen-PbI_2 mixture and cyclen powders. (b) Structure of cyclen-PbI_2-DMSO crystals. The downshift of the N-H stretching vibration frequency dues to the increase of electron cloud density triggered by hydrogen bonding with iodine (N-H…I).

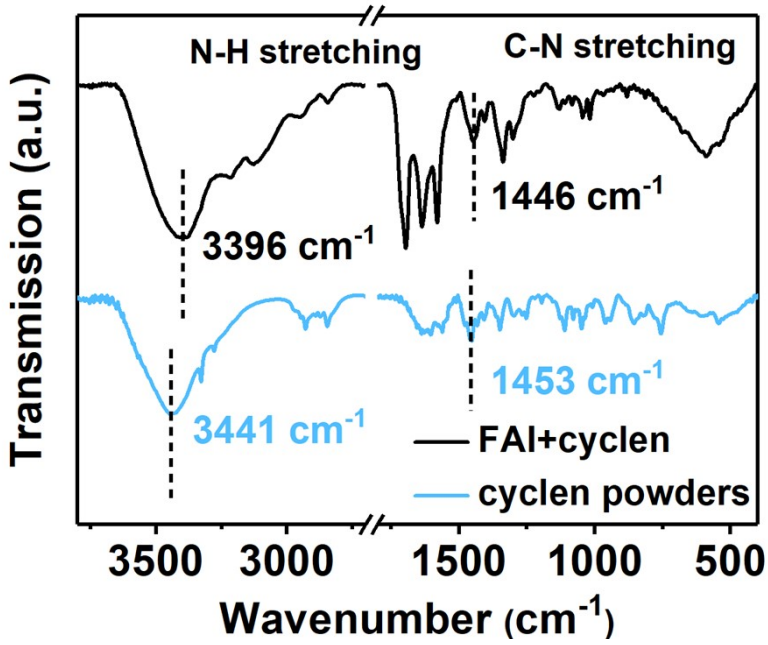

Figure S7. FTIR spectra of FAI-cyclen mixture and cyclen powders. The stretching vibration peaks of C-N bonds and N-H bonds in cyclen molecules shifted significantly after mixing. The peak of N-H bonds in cyclen shifted from 3441 cm^{-1} to 3396 cm^{-1} and the peak of C-N bond shifted from 1453 cm^{-1} to 1446 cm^{-1}, indicating that cyclen molecules can also interact with FAI, which can stabilize A-site cation in perovskite film.

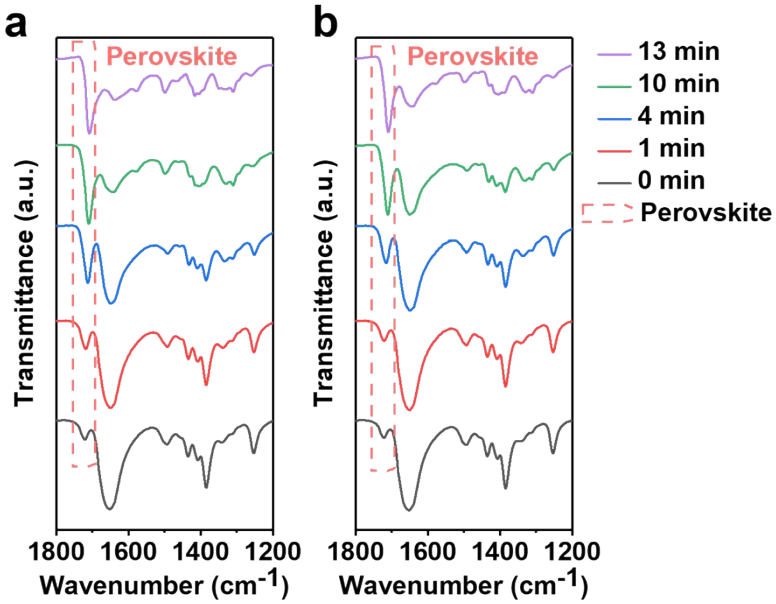

Figure S8. ATR-FTIR spectra of the local region of the (a) control and (b) cyclen-dopped precursor solution at different annealing duration.

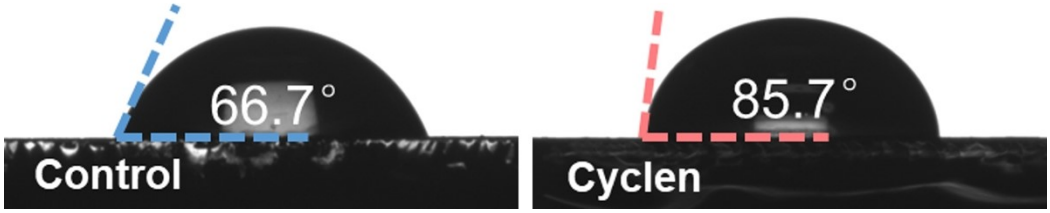

Figure S9. Water contact angles of the control and Cyclen films.

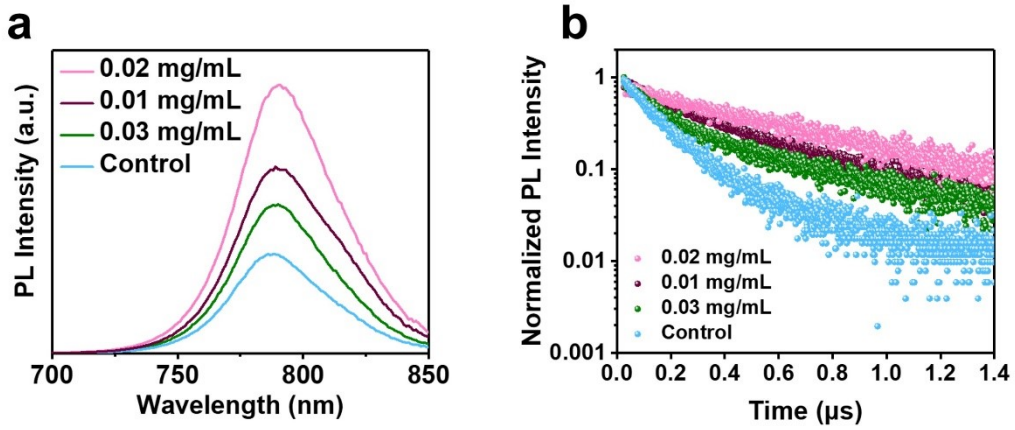

Figure S10. (a) PL and (b) TRPL spectra for the pristine perovskite films and with different concentrations of cyclen.

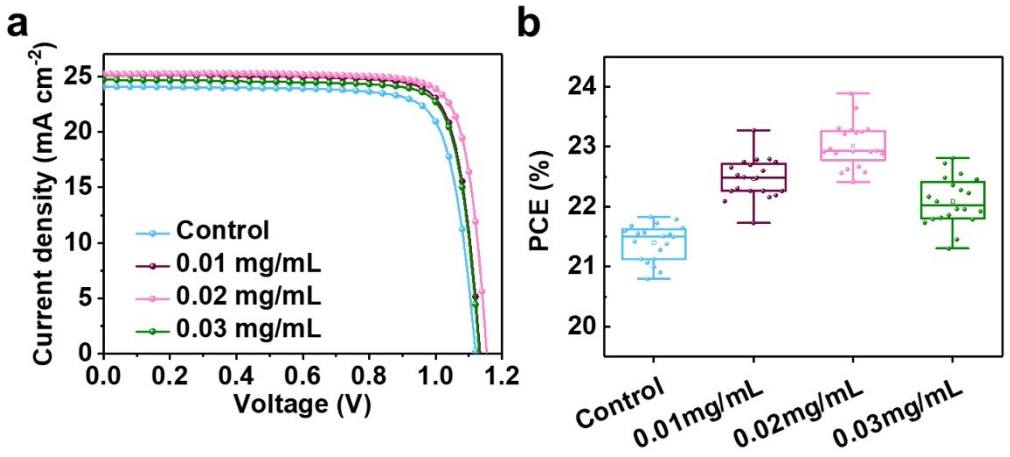

Figure S11. Device performance with CsFAMA-based perovskite films. (a) *J-V* curves of champion devices containing various concentrations of Cyclen. (b) Statistical results of PCE for 20 individual PSCs with various concentrations of cyclen.

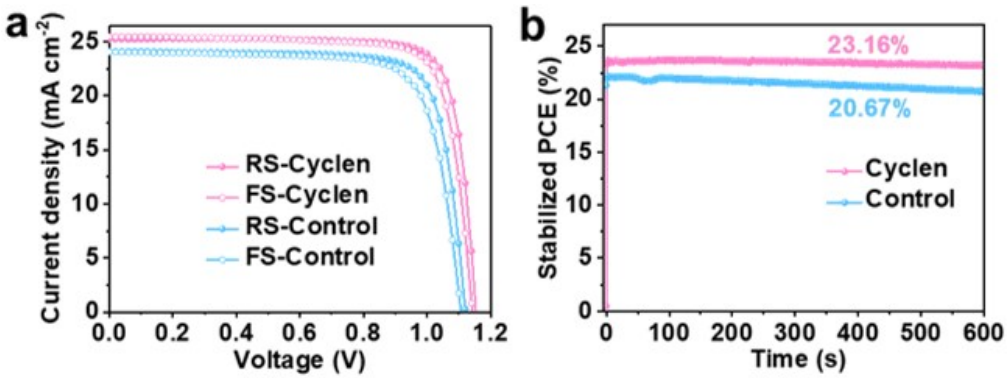

Figure S12. (a) *J-V* curves and (b) Stabilized PCEs of the champion control and Cyclen devices with CsFAMA perovskite films. The champion Cyclen device showed PCEs of 23.16%, while the control device displayed PCEs of 21.47%. Cyclen device exhibited more stable output, indicating fewer trap states in this device.

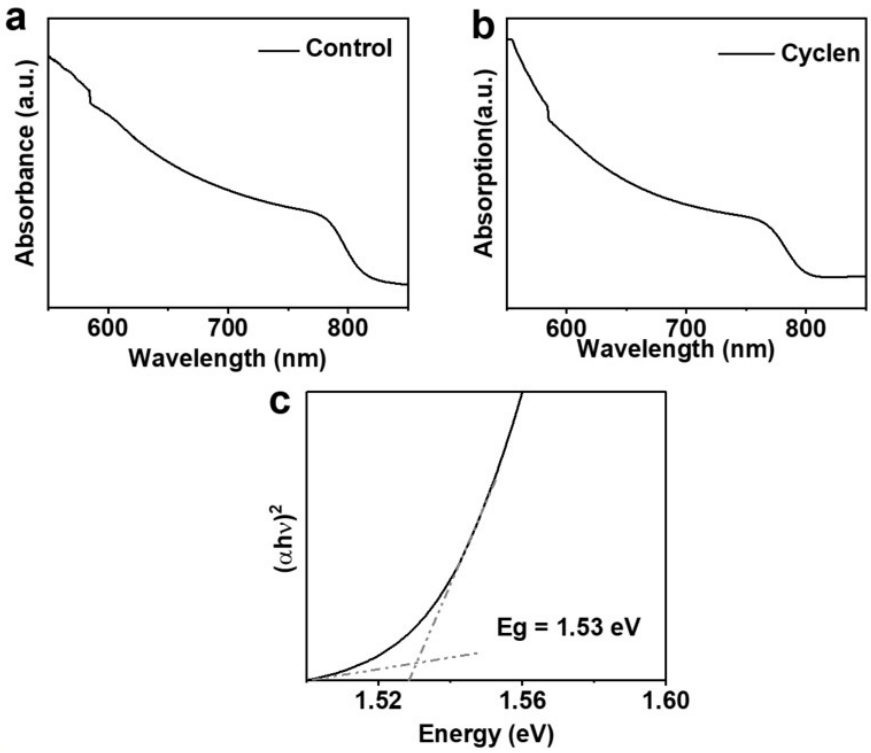

Figure S13. (a) and (b) UV-vis absorption spectra of control and cyclic modified $FAPbI_3$ perovskite films. (c) Optical bandgap estimation by the Tauc plot for the corresponding $FAPbI_3$ films.

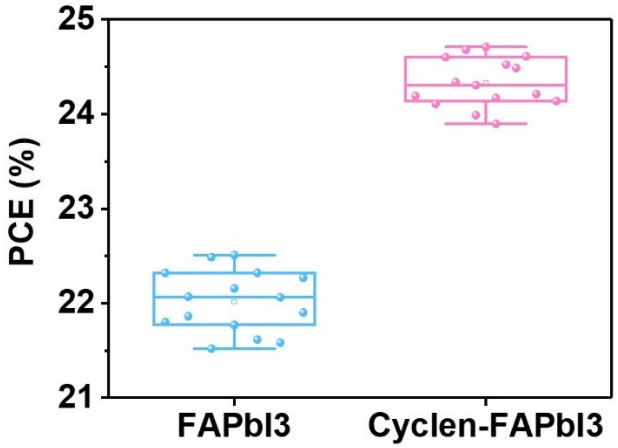

Figure S14. Statistical results of PCEs for 15 individual $FAPbI_3$ devices with and without cyclen.

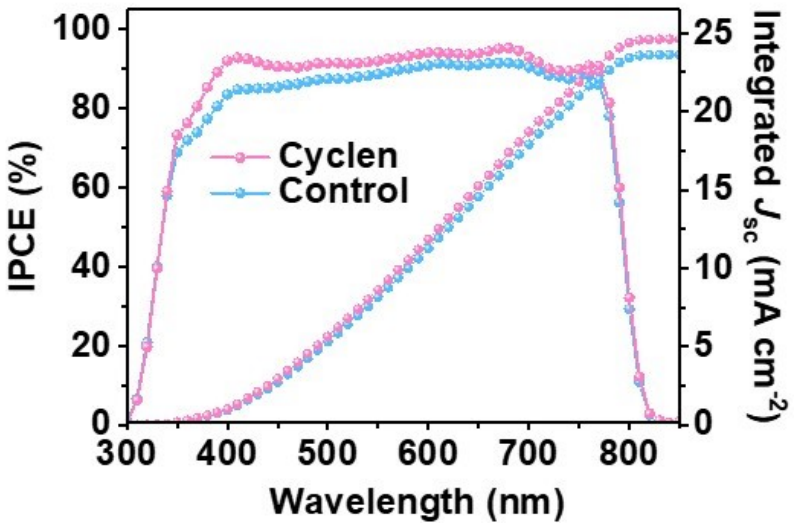

Figure S15. EQE spectra and the integrated J_{sc} curves of the champion control and Cyclen CsFAMA PSCs. According to the EQE spectra, the integrated J_{sc} of the champion Cyclen device was 24.62 mA cm^{-2}, which was higher than the control device (23.61 mA cm^{-2}), agreed well with the J_{sc} values from the above *J-V* curves.

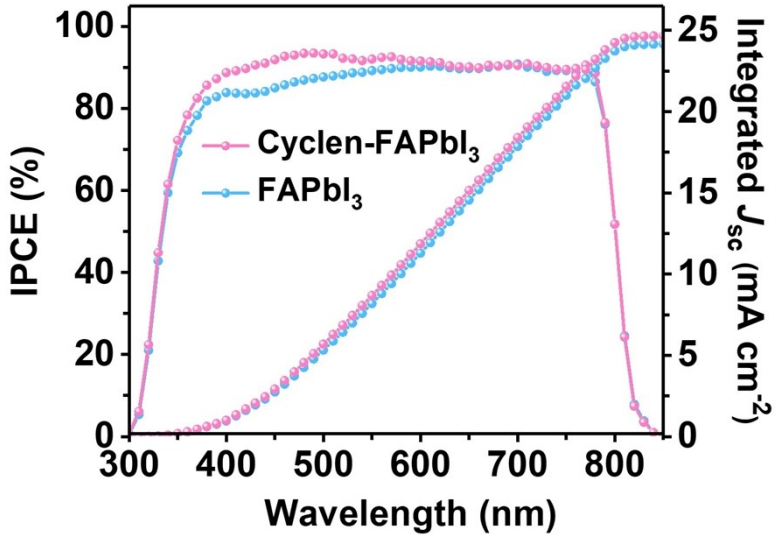

Figure S16. EQE spectra and the integrated J_{sc} curves of the champion control and Cyclen devices with $FAPbI_3$ perovskite films. According to the EQE spectra, the integrated J_{sc} of the champion Cyclen-$FAPbI_3$ device was 24.66 mA cm^{-2}, which was higher than the control device (24.15 mA cm^{-2}), agreed well with the J_{sc} values from the above *J-V* curves

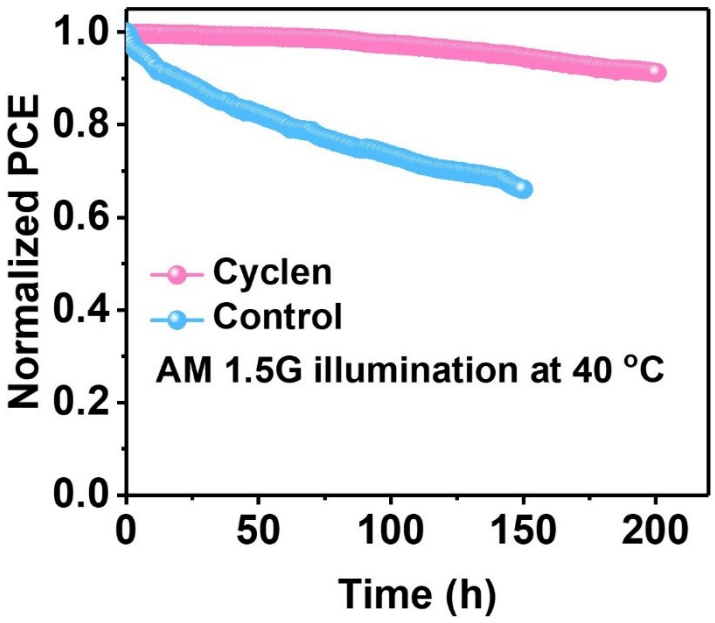

Figure S17. Light stability of the unencapsulated Cyclen and control devices under AM 1.5G illumination at 40 °C.

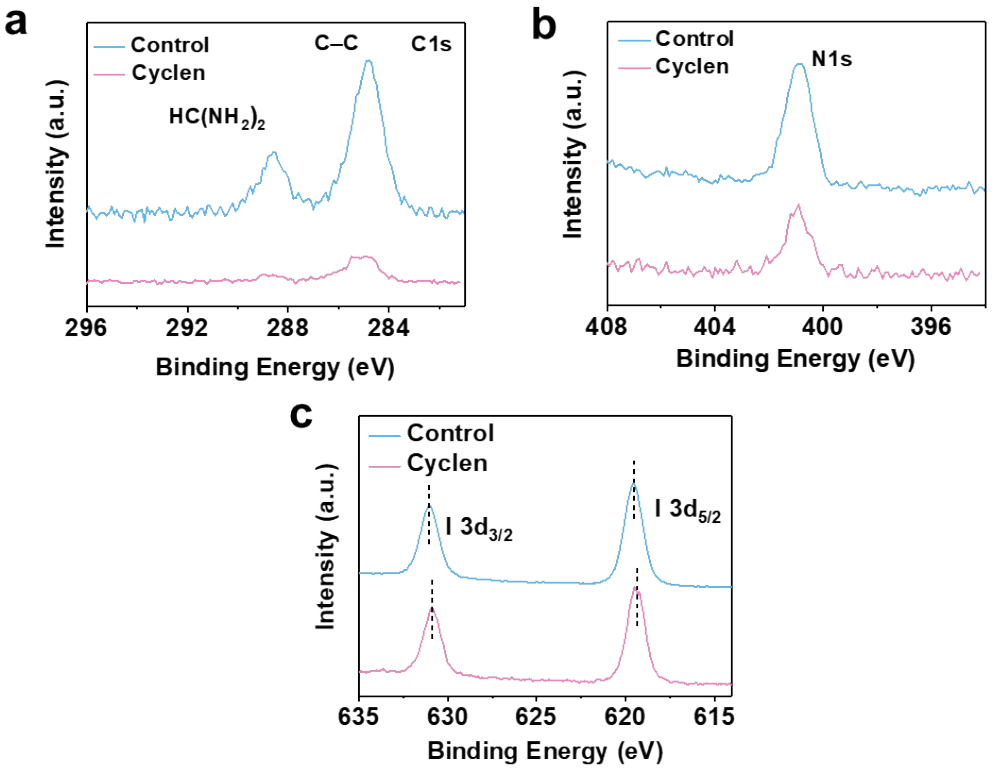

Figure S18. (a) C 1s, (b) N 1s and (c) I 3d XPS spectra for the control and Cyclen perovskite films.

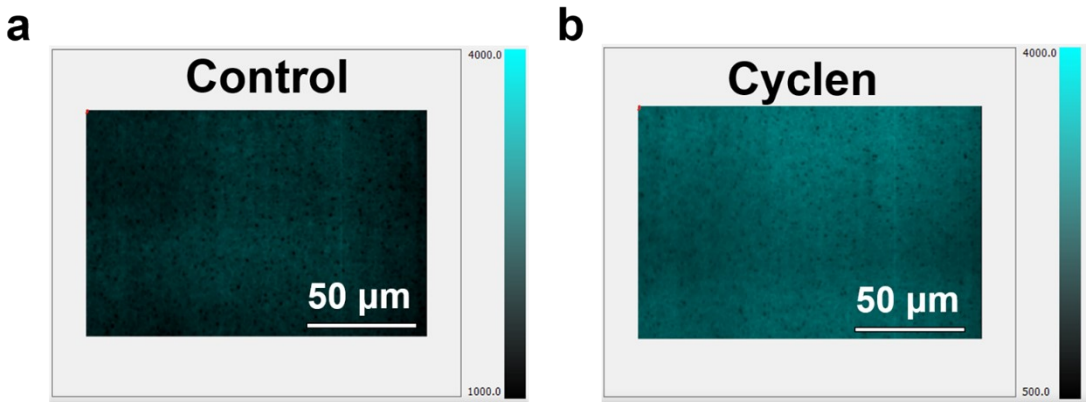

Figure S19. PL mapping of the control (a) and Cyclen (b) perovskite films.

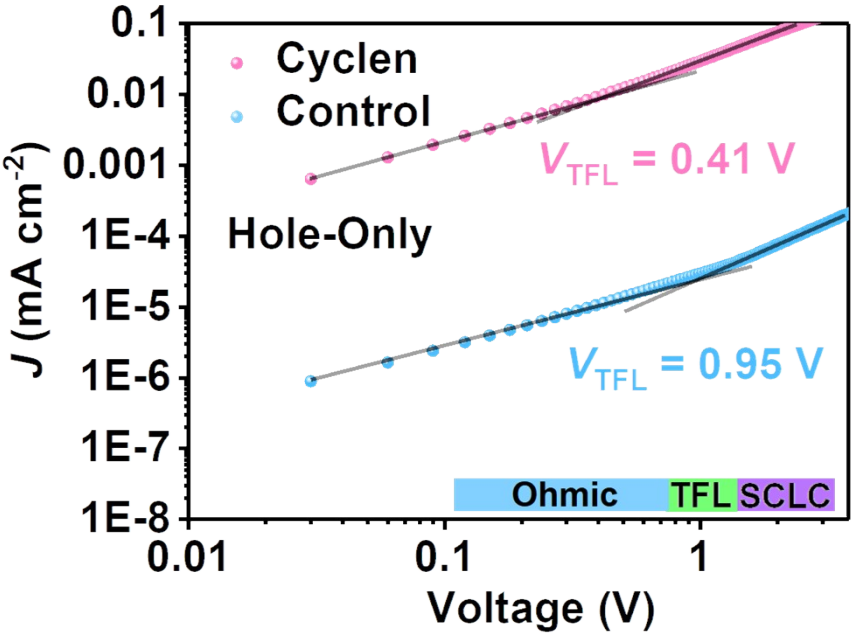

Figure S20. Dark *J-V* curves of the hole-only control and Cyclen devices.

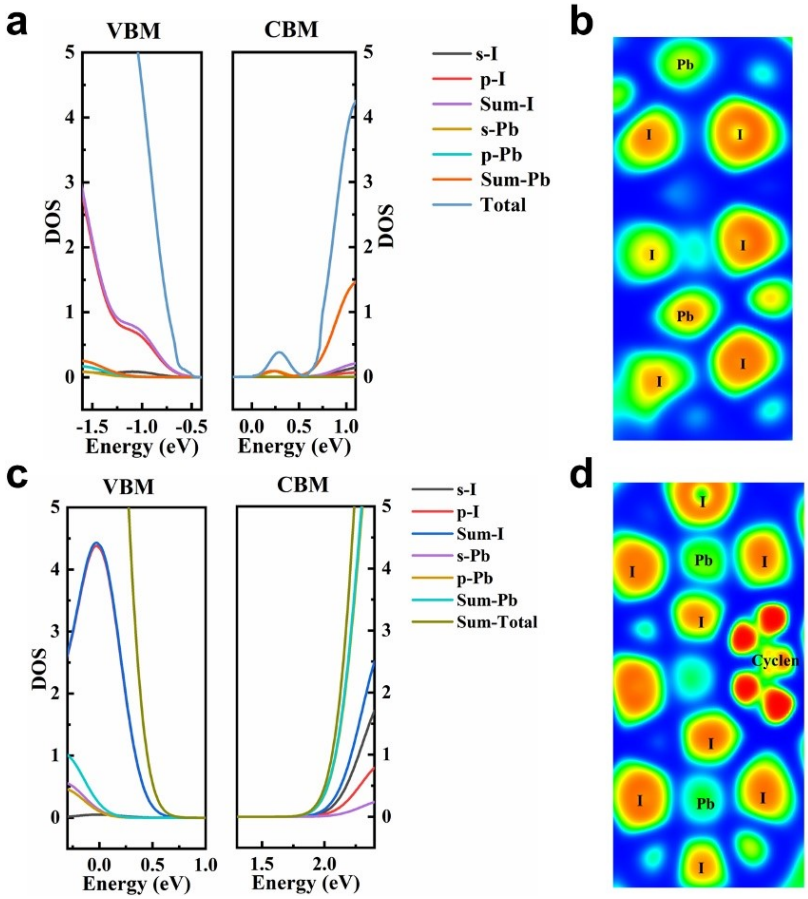

Figure S21. Electronic DOS curves of VBM and CBM of the control (a) and Cyclen (c) perovskite films. Electron localization function results of the control (b) and Cyclen (d) perovskite films.

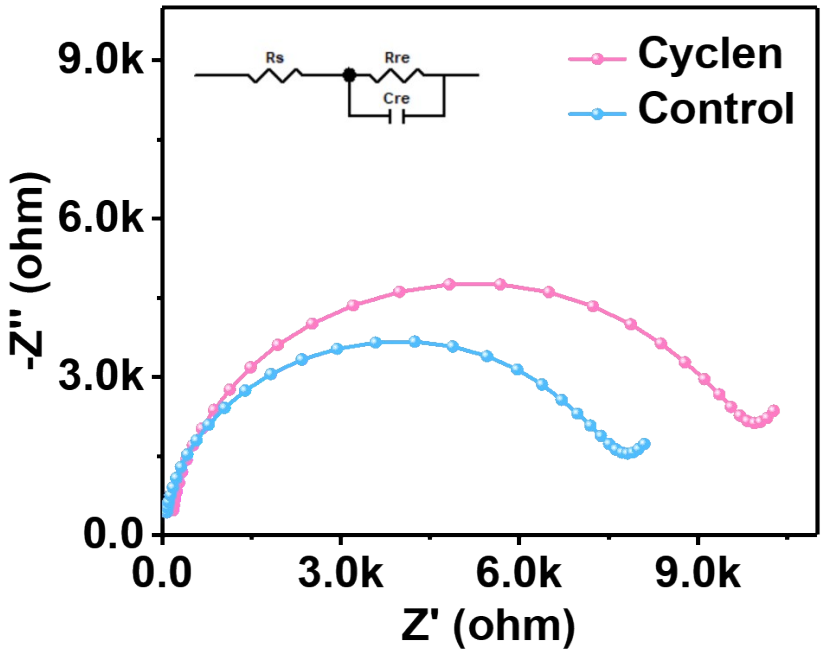

Figure S22. EIS of the control and Cyclen devices under 0.8 V in the dark condition. The semicircle corresponds to recombination resistance (R_{rec}). The Cyclen device exhibits an increased R_{rec} from 7727 to 9901 Ω, which significantly assisted the smoother charge carrier transport between perovskite and Spiro-OMeTAD and effectively suppressed nonradiative recombination loss, contributing to the higher V_{oc} and FF.

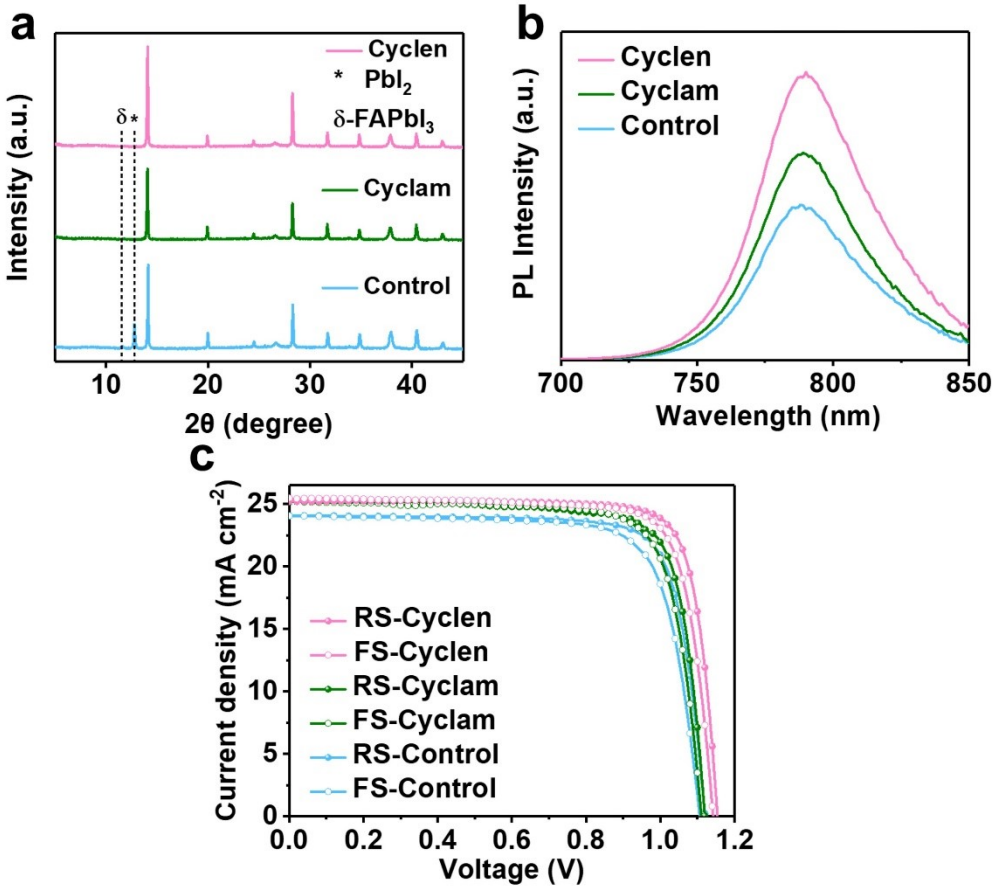

Figure S23. Cyclam comparison. (a) XRD patterns and (b) PL spectra of cyclen-passivated, cyclam-passivated and control perovskite films. (c) *J-V* curves of champion devices with or without cyclen and cyclam molecules.

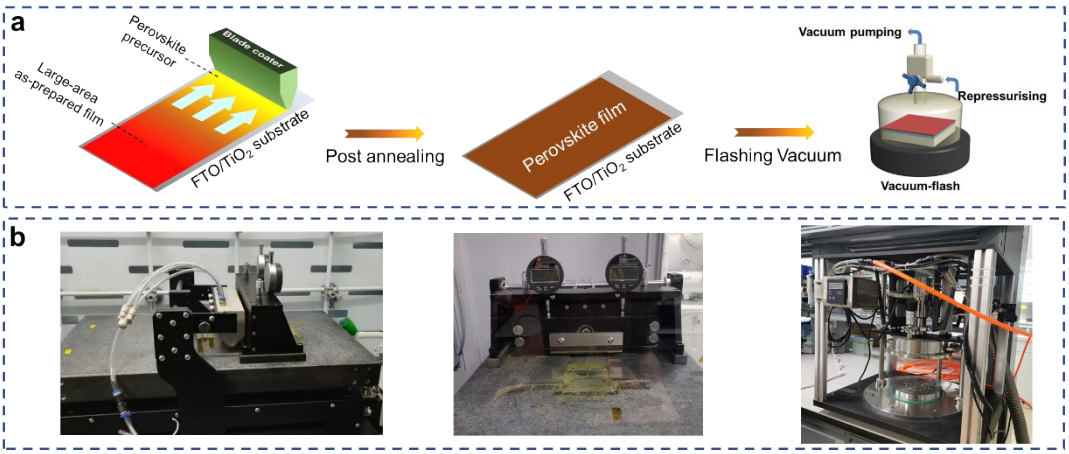

Figure S24. (a) Schematic of the fabrication process of the large-area perovskite film by blading coating. (b) Digital photos of the blade coater and vacuum chamber.

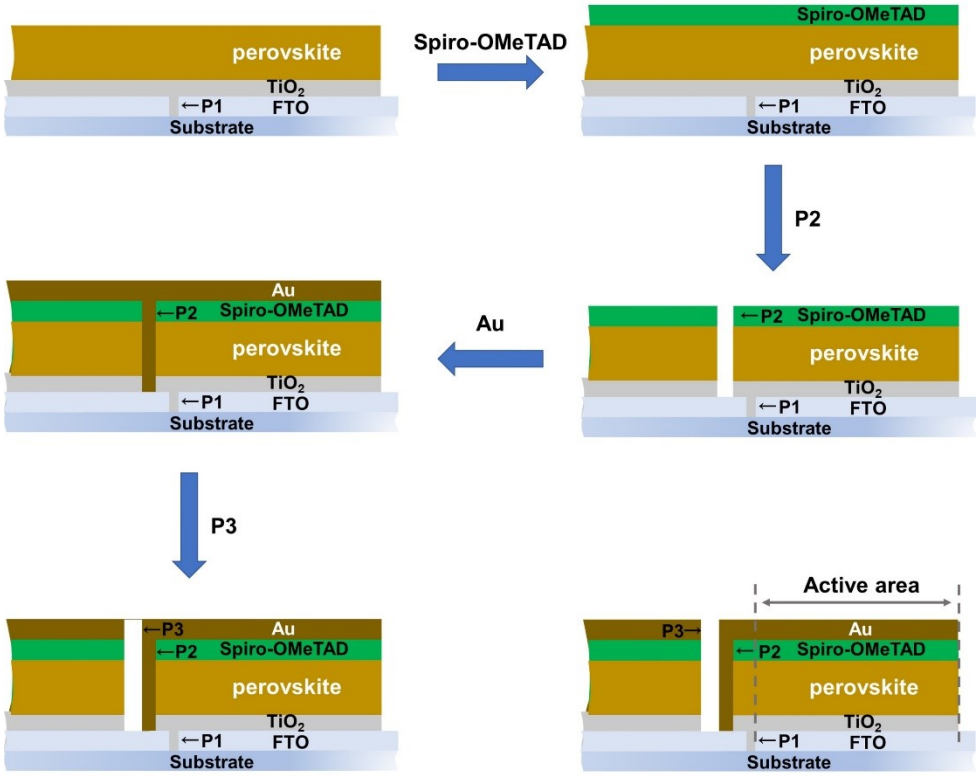

Figure S25. Schematic of the laser-scribing (P1, P2, P3) process for PSC module.

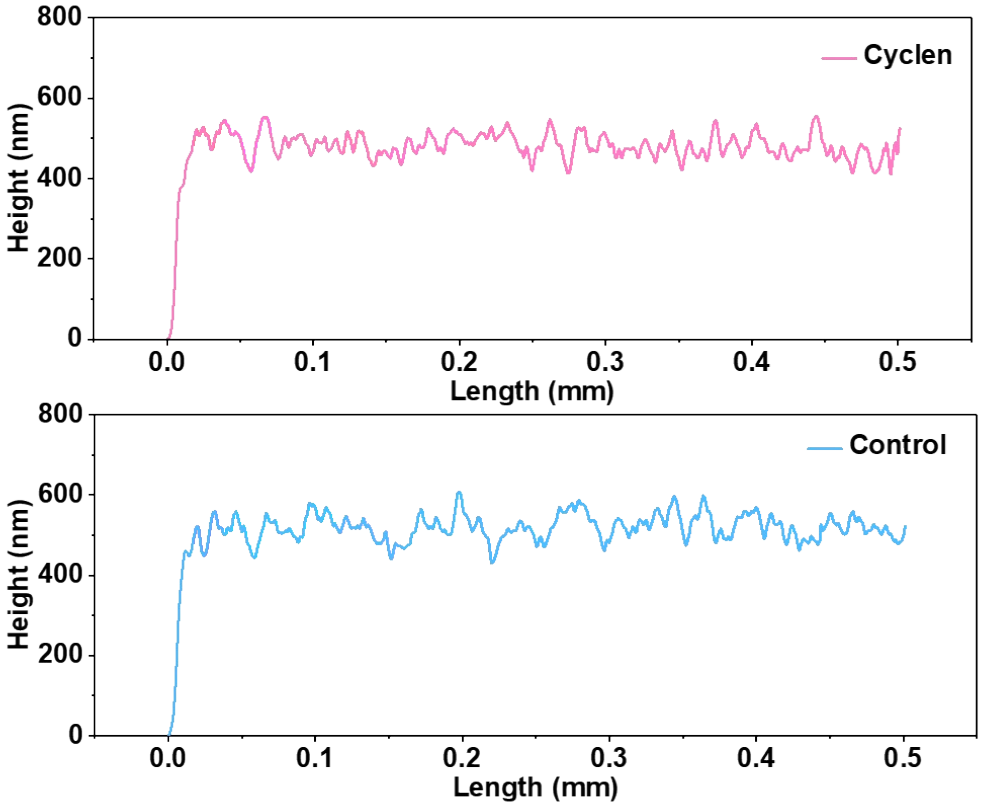

Figure S26. Surface profile measurement for the 36-cm^2 area Cyclen and Control films.

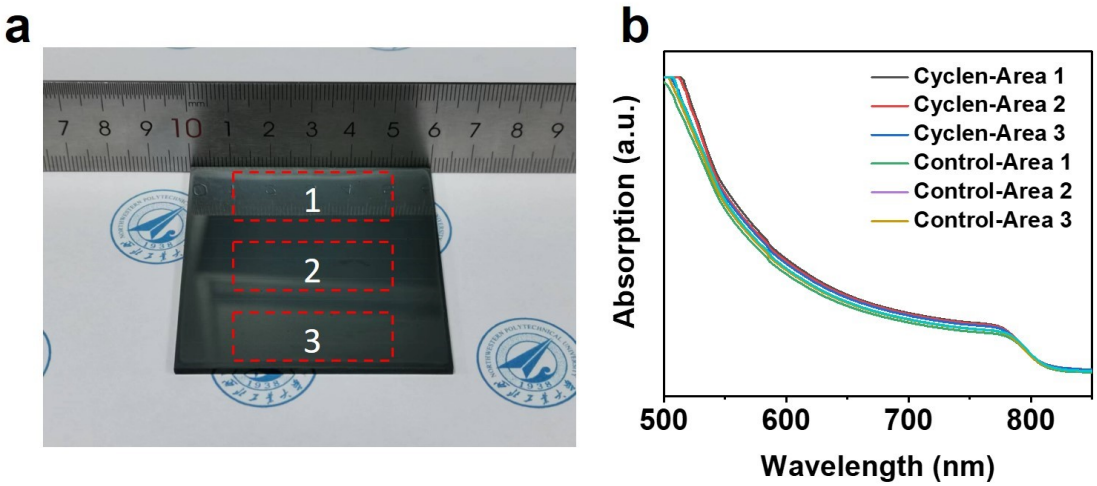

Figure S27. (a) Digital image of a large-area (36 cm^2) Cyclen film on TiO_2/FTO and (b) corresponding absorption spectra from the selected three different area within the film.

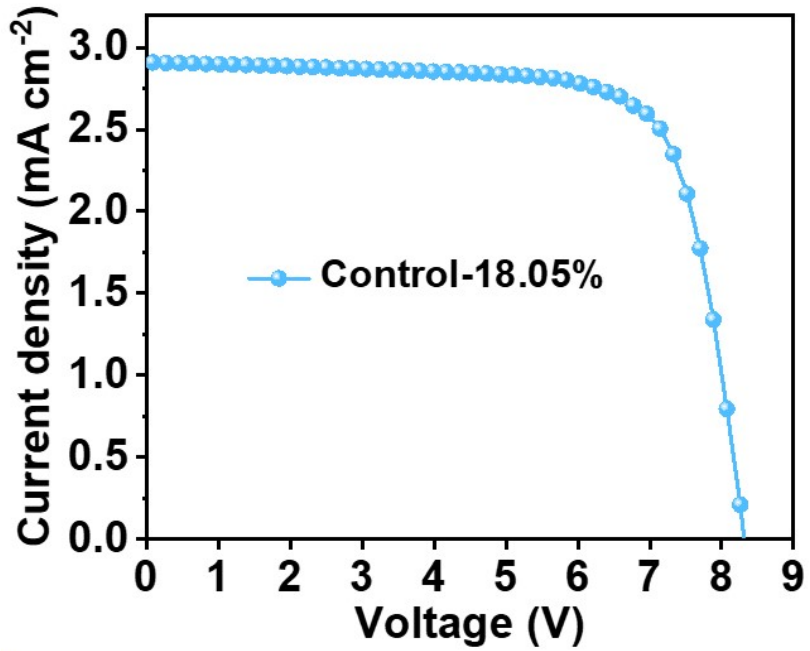

Figure S28. *J-V* curves of the control PSC module.

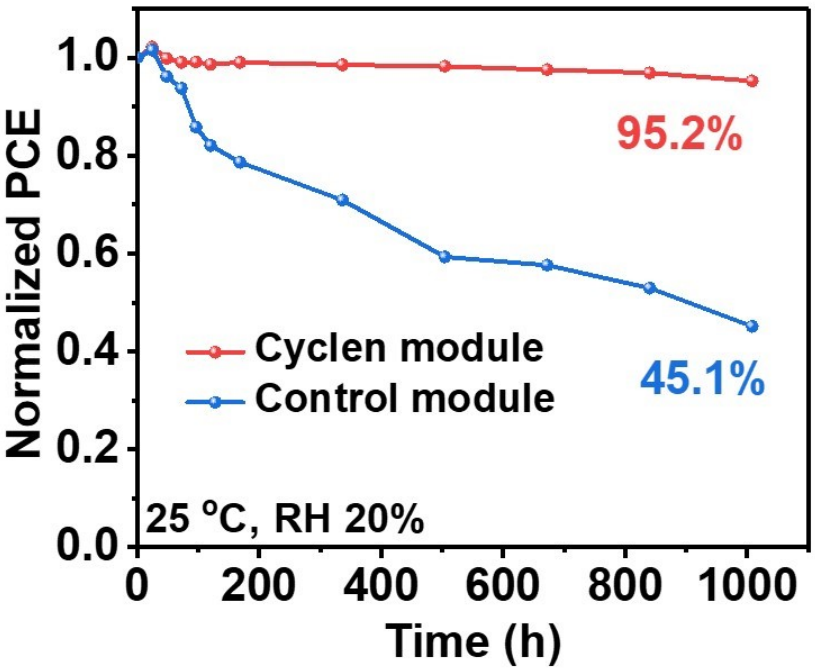

Figure S29. Long-term stability of the unencapsulated control and Cyclen PSC modules.

Table S1. Crystal data and structure refinement for cyclen-PbI_2-DMSO.

CCDC number	2221271
Empirical formula	$C_{10}H_{26}I_2N_4OPbS$
Formula weight	711.4
Temperature/K	100(2)
Crystal system	triclinic
Space group	*P-1*
a/Å	8.4396(4)
b/Å	8.5984(4)
c/Å	13.4137(7)
α/°	87.733(4)
β/°	77.448(4)
γ/°	82.384(4)
Volume/Å^3	941.69(8)
Z	2
ρ_{calc}g/cm^3	2.09
F(000)	652.0
Radiation	CuK\a (λ = 1.54184)
2Θ range for data collection/°	6.752 to 129.438
Index ranges	$-8 \le h \le 9$, $-7 \le k \le 9$, $-15 \le l \le 15$
Reflections collected	5553
Independent reflections	3095 [R_{int} = 0.0352, R_{sigma} = 0.0350]
Data/restraints/parameters	3095/6/174
Goodness-of-fit on F^2	1.026
Final R indexes [I>=2σ(I)]	R1 = 0.0486, wR2 = 0.1287
Final R indexes [all data]	R1 = 0.0494, wR2 = 0.1298
Largest diff. peak/hole / e Å^{-3}	3.64/-2.18

Table S2. Selected bond lengths (Å) for compound cyclen-PbI_2-DMSO.

Parameter	value	Parameter	value
Pb01-N00A	2.498(7)	Pb01-N007	2.563(7)
Pb01-N006	2.537(7)	Pb01-N008	2.574(7)

Table S3. Photovoltaic parameters of PSCs without/with different concentrations of cyclen molecules.

Sample	V_{oc} (V)	J_{sc} (mA cm^{-2})	*FF* (%)	PCE (%)
Control	1.121	24.08	79.52	21.47
0.01 mg/mL	1.134	25.16	81.10	23.14
0.02 mg/mL	1.154	25.22	82.10	23.90
0.03 mg/mL	1.132	24.70	81.52	22.79

Table S4. Photovoltaic parameters of control and Cyclen PSCs measured from forward scan and reverse scan.

Sample	V_{oc} (V)	J_{sc} (mA cm^{-2})	*FF* (%)	PCE (%)
Control-reverse	1.121	24.08	79.52	21.47
Control-forward	1.106	24.05	76.23	20.28
Cyclam-reverse	1.120	25.27	78.41	22.19
Cyclam-forward	1.111	25.17	77.65	21.71
Cyclen-reverse	1.154	25.22	82.10	23.90
Cyclen-forward	1.142	25.47	79.57	23.14

Table S5. Photovoltaic parameters of control and Cyclen PSCs based $FAPbI_3$ films.

Sample	V_{oc} (V)	J_{sc} (mA cm^{-2})	*FF* (%)	PCE (%)
Control-reverse	1.124	25.16	79.59	22.51
Control-forward	1.103	25.17	78.41	21.77
Cyclen-reverse	1.161	25.48	83.53	24.71
Cyclen-forward	1.153	25.42	82.45	24.17

Table S6. The reported PCE from PSCs with ring structure molecules.

Perovskite	Bandgap (eV)	Additive	Champion PCE (%)	V_{oc}	J_{sc}	FF	Ref.
$Cs_{0.05}(MA_{0.17}FA_{0.83})_{0.95}Pb(I_{0.83}Br_{0.17})_3$	~1.60	18-Crown-6 ether	20.73	1.170	23.67	74.80	[5]
$CsPbI_3$	~1.7	18-Crown-6 ether	16.90	1.060	20.56	77.61	[6]
$FA_{0.85}Cs_{0.15}PbI_3$	~1.54	Dibenzo-18-Crown-6 ether	20.84	1.110	23.84	78.75	[7]
$FA_{0.85}MA_{0.15}Pb(I_{0.85}Br_{0.15})_3$	~1.58	15-Crown-5 ether	21.50	1.160	24.15	76.60	[8]
$FA_{0.97}Cs_{0.03}PbI_3$	~1.53	18-Crown-6 ether	20.48	1.060	24.40	79.19	[4]
$FA_{0.97}MA_{0.03}PbI_{2.97}Br_{0.03}$	1.56	Dibenzo-24-Crown-8 ether	23.70	1.154	25.80	79.50	[9]
$(FAPbI_3)_{0.97}(MAPbBr_3)_{0.03}$	~1.56	Dibenzo-21-Crown-7 ether	24.30	1.170	25.50	81.90	[10]
$FA_{0.97}Cs_{0.04}MA_{0.03}Pb(I_{0.97}Br_{0.03})_3$	~1.57	1-aza-18-Crown-6 ether	24.07	1.174	24.95	82.15	[11]
$FAPbI_3$	**~1.53**	**Cyclen**	**24.71**	**1.161**	**25.48**	**83.53**	**This work**

Table S7. Photovoltaic parameters of Cyclen module with 36-cm^2 total area (18 cm^2 active area).

Sample	V_{oc} (V)	J_{sc} (mA cm^{-2})	*FF* (%)	PCE (%)
Control	8.30	2.91	74.73	18.05
Cyclen	8.83	2.96	76.82	20.08

References

[1] P. Guo, C. Liu, X. Li, Z. Chen, H. Zhu, L. Zhu, X. Zhang, W. Zhao, N. Jia, Q. Ye, X. Xu, R. Chen, Z. Liu, X. Fan, C. Zhi, H. Wang, *Adv. Energy Mater.* 2022, **12**, 2202395.

[2] H. Min, D. Y. Lee, J. Kim, G. Kim, K. S. Lee, J. Kim, M. J. Paik, Y. K. Kim, K. S. Kim, M. G. Kim, T. J. Shin, S. Il Seok, *Nature* 2021, **598**, 444-450.

[3] N. Jia, P. Guo, K. Zhang, C. Liu, R. Chen, Z. Liu, Q. Ye, H. Wang, *ACS Sustain. Chem. Engin.* 2022, **10**, 16359-16367.

[4] R. Chen, Y. Wu, Y. Wang, R. Xu, R. He, Y. Fan, X. Huang, J. Yin, B. Wu, J. Li, N. Zheng, *Adv. Funct. Mater.* 2021, **31**, 2008760.

[5] X. Wu, Y. Jiang, C. Chen, J. Guo, X. Kong, Y. Feng, S. Wu, X. Gao, X. Lu, Q. Wang, G. Zhou, Y. Chen, J.-M. Liu, K. Kempa, J. Gao, *Adv. Func. Mater.* 2020, **30**, 1908613.

[6] R. Chen, Y. Hui, B. Wu, Y. Wang, X. Huang, Z. Xu, P. Ruan, W. Zhang, F. Cheng, W. Zhang, J. Yin, J. Li, N. Zheng, *J. Mater. Chem. A* 2020, **8**, 9597-9606.

[7] X. Sun, F. Deng, S. Li, Y. Li, X. Lv, Y.-Z. Zheng, X. Tao, *Sol. RRL* 2022, **6**, 2200303.

[8] P. Gao, Y. Ji, J. Song, G. Zhou, J. Lai, X. Yin, Y. Li, T. Song, Z. Zhao, Q. Chen, W. Feng, L. Chen, Y. Zhang, S. Yang, B. Sun, F. Liu, *Cell Reports Physical Science* 2021, **2**, 100450.

[9] T.-S. Su, F. T. Eickemeyer, M. A. Hope, F. Jahanbakhshi, M. Mladenović, J. Li, Z. Zhou, A. Mishra, J.-H. Yum, D. Ren, A. Krishna, O. Ouellette, T.-C. Wei, H. Zhou, H.-H. Huang, M. D. Mensi, K. Sivula, S. M. Zakeeruddin, J. V. Milić, A. Hagfeldt, U. Rothlisberger, L. Emsley, H. Zhang, M. Grätzel, *J. Am. Chem. Soc.* 2020, **142**, 19980-19991.

[10] H. Zhang, F. T. Eickemeyer, Z. Zhou, M. Mladenović, F. Jahanbakhshi, L. Merten, A. Hinderhofer, M. A. Hope, O. Ouellette, A. Mishra, P. Ahlawat, D. Ren, T.-S. Su, A. Krishna, Z. Wang, Z. Dong, J. Guo, S. M. Zakeeruddin, F. Schreiber, A. Hagfeldt, L. Emsley, U. Rothlisberger, J. V. Milić, M. Grätzel, *Nat. Commun.* 2021, **12**, 3383.

[11] Y. Yang, T. Zhao, M.-H. Li, X. Wu, M. Han, S.-C. Yang, Q. Xu, L. Xian, X. Chi, N.-J. Zhao, H. Cui, S. Li, J.-S. Hu, B. Zhang, Y. Jiang, *Chem. Engin. J.* 2023, **451**, 138962.